# Density Scaling of Noninteracting Kinetic Energy Functionals

Alex Borgoo* and David J. Tozer*

Department of Chemistry, Durham University, South Road, Durham DH1 3LE, United Kingdom

ABSTRACT: The influence of imposing an approximate density scaling condition on a noninteracting kinetic energy functional is investigated. A simple generalized gradient approximation (GGA) is presented, which satisfies both the density scaling condition and the usual coordinate scaling condition; the remaining multiplicative constant is determined from an energy criterion. In post-Kohn−Sham calculations, noninteracting kinetic energies of the closed-shell molecules of the G1 set determined using the GGA are a modest improvement over those determined using the corresponding local functional, which does not satisfy the density scaling condition. Potential energy curves of CO, F_2, and P_2 exhibit binding with the GGA, compared to purely repulsive curves with the local functional. Adjusting the exponent in the GGA form in order to optimize energy accuracy violates the density scaling condition, and two of the diatomics no longer exhibit binding. Results are compared with those from other local/GGA functionals in the literature.
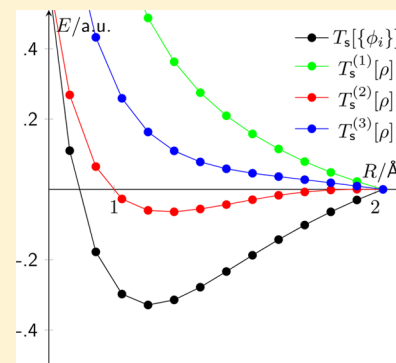
■ INTRODUCTION

Kohn−Sham[1] density functional theory[2] (DFT) is the most widely used method for determining the electronic structure of molecules and solids. Despite the cost effectiveness of the method, very large systems remain intractable due to the reliance on one-electron orbitals, which are used in the evaluation of the noninteracting kinetic energy

$$T_s[\{\phi_i\}] = -\frac{1}{2} \sum_i \int \phi_i(\mathbf{r}) \, \nabla^2 \, \phi_i(\mathbf{r}) \, d\mathbf{r} \tag{1}$$

where $\{\phi_i(\mathbf{r})\}$ are occupied orbitals. This term is a key component of the total electronic energy functional

$$E[\rho] = T_s[\{\phi_i\}] + \int v_{ext}(\mathbf{r}) \, \rho(\mathbf{r}) \, d\mathbf{r} + J[\rho] + E_{xc}[\rho] + E_n \tag{2}$$

where $v_{ext}(\mathbf{r})$ is the external potential, $\rho(\mathbf{r})$ is the electron density, $J[\rho]$ is the classical Coulomb interaction energy, $E_{xc}[\rho]$ is the exchange−correlation energy, and E_n is the nuclear repulsion energy.

A desirable way forward would be to eliminate the orbitals and construct a theory that depends on the density alone, formally reducing the computational cost from cubic to quasi-linear. This requires the exact orbital functional $T_s[\{\phi_i\}]$ in eqs 1 and 2 to be replaced by an explicit density functional $T_s[\rho]$, a challenge that has been the subject of much research. The problem is that $T_s[\rho]$ has a large magnitude, and so even small percentage errors are problematic. Noninteracting kinetic energy functionals also play an important role in frozen density embedding approaches.[3−5]

Many approximations for $T_s[\rho]$ have been proposed, ranging in complexity from the simple Thomas−Fermi uniform electron gas approximation[6,7] to nonlocal approximations (e.g., see refs 8, 9, and references therein). Of particular relevance to the present study are generalized gradient approximations (GGA), which depend on the density and its gradient. Many GGAs have been proposed,[10−23] largely based on the conjointness argument of Lee, Lee, and Parr,[10] which states that the enhancement factor for a noninteracting kinetic energy functional should have the same analytic form as that of an exchange functional.

A common approach in DFT functional development is to impose known coordinate scaling conditions.[24] The aim of the present study is to investigate the influence of imposing an additional, approximate *density* scaling condition, based on observations that we made recently in ref 25. We commence by reviewing the relevant scaling/homogeneity properties of functionals and show how these may be imposed. The results of our numerical trials are then discussed and conclusions are drawn.

■ THEORETICAL DETAILS

Homogeneity under Coordinate Scaling and Density Scaling. A functional $F[\rho]$ is homogeneous of degree m under *coordinate scaling* if it satisfies[24]

$$F[\rho_\lambda] = \lambda^m F[\rho] \tag{3}$$

where the electronic coordinate is scaled by a factor λ and the scaled density is defined as

$$\rho_\lambda(\mathbf{r}) = \lambda^3 \rho(\lambda \mathbf{r}) \tag{4}$$

maintaining normalization to the number of electrons N

$$\int \rho_\lambda(\mathbf{r}) \, d\mathbf{r} = \int \rho(\mathbf{r}) \, d\mathbf{r} = N \tag{5}$$

The exact noninteracting kinetic energy is homogeneous of degree 2 under coordinate scaling; this condition will be imposed throughout the present study.

A functional $F[\rho]$ is homogeneous of degree k under *density scaling* if it satisfies

$$F[\xi\rho] = \xi^k F[\rho] \tag{6}$$

where the density has been scaled by a factor ξ. For $k \neq 0$, this leads to the familiar relationship[26]

$$k = \frac{\int \rho(\mathbf{r}) \frac{\delta F[\rho]}{\delta \rho(r)} \, d\mathbf{r}}{F[\rho]} \tag{7}$$

This ratio can still be evaluated for nonhomogeneous functionals, but then k becomes system-dependent. Following Zhao et al.,[27] we term this system-dependent quantity an "effective homogeneity" and denote it k_{eff}. In a recent study,[25] we used experimental and near-exact calculated data to investigate the homogeneity properties under density scaling of the exact noninteracting kinetic energy functional. For a series of atoms and small molecules, we concluded that the functional was not homogeneous of any degree but that the effective homogeneity associated with the potential that averages over the integer discontinuity—which is most appropriate for a continuum functional such as a GGA—did not exhibit significant system dependence for systems with more than one electron. We denote these near-exact effective homogeneities by k_{eff}^0.

Imposing Coordinate and Density Scaling Homogeneity. First consider a local functional of the form

$$T_s[\rho] = \alpha \int \rho^k(\mathbf{r}) \, d\mathbf{r} \tag{8}$$

which is homogeneous of degree

$$m = 3k - 3 \tag{9}$$

under coordinate scaling and homogeneous of degree k under density scaling. Imposing the coordinate scaling condition ($m = 2$) necessitates that $k = 5/3$, as in the familiar Thomas–Fermi expression. For the purpose of the present study, we denote this Thomas–Fermi-type approximation as

$$T_s^{(1)}[\rho] = \alpha \int \rho^{5/3}(\mathbf{r}) \, d\mathbf{r} \tag{10}$$

where α is to be determined. Multiplicative constants such as α cannot, of course, be determined from scaling considerations; Parr and Yang have commented on the nonsacrosanct nature of these constants.[2]

In order to impose an additional density scaling condition, while maintaining the coordinate scaling condition, we consider the more flexible GGA form

$$T_s[\rho] = \beta \int \rho^{5/3}(\mathbf{r}) \, x^q(\mathbf{r}) \, d\mathbf{r} \tag{11}$$

where $x = |(\nabla \rho)|/\rho^{4/3}$ is dimensionless. Like eq 10, this is homogeneous of degree 2 under coordinate scaling for all values of q. However, it is homogeneous of degree

$$k = \frac{1}{3}(5 - q) \tag{12}$$

under density scaling, meaning any desired homogeneity can be imposed through an appropriate choice of q. We note that using $q = 2$ returns the von Weizsäcker functional form,[28]

which is also the form of the leading correction in the gradient expansion.

A natural way forward would therefore be to choose q in eq 12 such that k equals the near-exact effective homogeneity k_{eff}^0 from ref 25, but such a functional would be system-dependent, due to the system-dependence of k_{eff}^0. To obtain a system-independent functional, we instead determine the average value of k_{eff}^0, denoted $k_{\text{eff,av}}^0$, for the set of closed-shell atoms and molecules in ref 25, namely, He, Be, Ne, Mg, Ar, Ca, SO_2, Cl_2, F_2, CO, PH_3, H_2S, N_2, HCl, NH_3, HF, H_2O, and CH_4, which exhibit k_{eff}^0 values in the range from 1.5 to 1.6. We then use this average value to determine the exponent

$$q_{\text{av}} = 5 - 3k_{\text{eff,av}}^0 = 0.3434125 \tag{13}$$

noting that q_{av} is simply the average of the system-dependent q values. We denote this GGA approximation as

$$T_s^{(2)}[\rho] = \beta \int \rho^{5/3}(r) \, x^{q_{\text{av}}}(\mathbf{r}) \, d\mathbf{r} \tag{14}$$

We note that our procedure could be easily generalized to a meta-GGA form, depending on the higher-order dimensionless parameter; test calculations suggest that a meta-GGA leads to similar conclusions as a GGA. The functionals could also be generalized to a spin-polarized framework as follows[29]

$$T_s[\rho_\uparrow, \rho_\downarrow] = 1/2(T_s[2\rho_\uparrow] + T_s[2\rho_\downarrow]) \tag{15}$$

where $\rho_\uparrow$ and $\rho_\downarrow$ are the spin densities.

■ NUMERICAL TRIALS

All calculations using approximate noninteracting kinetic energy functionals are performed in a post-Kohn–Sham manner, using densities determined using the Perdew–Burke–Ernzerhof (PBE) exchange-correlation functional[30] and the aug-cc-pVTZ basis set.[31−33] These densities approximate those that would be obtained from a solution of the Euler equation using the exact $T_s[\rho]$. Such a post-Kohn–Sham approach has been used in many previous studies, e.g., see refs 23, 34−36. The accuracy of the results is quantified by comparing with the Kohn–Sham results. All calculations use a spin-restricted formalism.

For the functional $T_s^{(1)}[\rho]$ in eq 10, we define the optimal parameter α from the zero intercept linear regression between the quantity $T_s^{(1)}[\rho]/\alpha = \int \rho^{5/3}(\mathbf{r}) \, d\mathbf{r}$ and the Kohn–Sham $T_s[\{\phi_i\}]$ in eq 1, for the closed-shell systems of ref 25 at the same[37] reference geometries. An optimal value of $\alpha = 3.099189$ is obtained, corresponding to a mean absolute percentage error for these systems of 1.5%. For the functional $T_s^{(2)}[\rho]$ in eq 14, the analogous procedure yields an optimal value of $\beta = 1.990328$, corresponding to a mean absolute percentage error of 1.3%.

To quantify the accuracy of the resulting $T_s^{(1)}[\rho]$ and $T_s^{(2)}[\rho]$ for systems beyond those in the fitting set of ref 25, we have determined $T_s[\rho]$ values for the 37 closed-shell molecules of the G1 set, using MP2/6-31G(d) geometries. Table 1 presents the slope and intercept of the correlation between the approximate $T_s[\rho]$ and Kohn–Sham $T_s[\{\phi_i\}]$, together with mean absolute errors (MAEs) and mean absolute percentage errors (MAPEs) over the set. In moving from $T_s^{(1)}[\rho]$ to $T_s^{(2)}[\rho]$, all the quantities improve slightly.

Figure 1 plots the error and percentage error in $T_s^{(1)}[\rho]$ and $T_s^{(2)}[\rho]$, as a function of the Kohn–Sham $T_s[\{\phi_i\}]$ for these G1 molecules; for both functionals, the largest error occurs for the

Table 1. Slope (m) and Intercept (c) for the Correlation between Approximate $T_s[\rho]$ and Kohn–Sham $T_s[\{\phi_i\}]$ for Closed-Shell Molecules in the G1 Set[a]

	m	c/au	MAE/au	MAPE
$T_s^{(1)}[\rho]$	0.997	2.269	1.680	1.362
$T_s^{(2)}[\rho]$	1.002	−1.749	1.472	1.183
$T_s^{(3)}[\rho]$	1.000	−0.029	0.210	0.130
$T_s^{TF}[\rho]$	1.076	2.269	21.359	8.585
$T_s^{T92}[\rho]$	1.000	0.171	0.257	0.178
$T_s^{PBE2}[\rho]$	0.640	−7.434	164.647	64.976

[a]In all cases, the correlation coefficient is 1.000. Also shown are the mean absolute error (MAE) and mean absolute percentage error (MAPE).

CH₃SH molecule. It is clear that $T_s^{(1)}[\rho]$ and $T_s^{(2)}[\rho]$ generally underestimate and overestimate, respectively, suggesting that an intermediate functional might yield improved results. Notwithstanding the fact that such a functional would violate the density scaling condition of eq 13, it is of interest to quantify just how accurately the energy can be reproduced. Investigations indicated that the use of an intermediate exponent of $q_{opt} = 0.2$, corresponding to a homogeneity of $k = 1.6$, yields near-optimal energies for the G1 set. We denote this functional

$$T_s^{(3)}[\rho] = \gamma \int \rho^{5/3}(\mathbf{r}) \, x^{q_{opt}}(\mathbf{r}) \, d\mathbf{r} \tag{16}$$

where the optimal value of $\gamma = 2.397888$ was determined as before, corresponding to a mean absolute percentage error of 0.1% for the fitting set of ref 25. Results for the G1 molecules determined using $T_s^{(3)}[\rho]$ are presented in Table 1 and Figure 1. The functional yields significantly more accurate energies than both $T_s^{(1)}[\rho]$ and $T_s^{(2)}[\rho]$. The situation bears some analogy with our recent study of negative electron affinities, where imposing a theoretically motivated homogeneity also overcompensated the errors.[38]

To put the results from the new functionals into some perspective, we also consider the performance of three representative local/GGA functionals, namely the Thomas–Fermi local functional, denoted $T_s^{TF}[\rho]$, the T92 GGA functional of Thakkar,[22] denoted $T_s^{T92}[\rho]$, and the PBE2 GGA functional of Karasiev et al.,[13,23] denoted $T_s^{PBE2}[\rho]$. Results for the closed-shell G1 molecules are presented in Table 1. $T_s^{(1)}[\rho]$ is a notable improvement over $T_s^{TF}[\rho]$,

illustrating the effect of varying the multiplicative constant. $T_s^{(2)}[\rho]$ is notably more accurate than $T_s^{PBE2}[\rho]$, which can be traced to the fact that the latter was developed with an emphasis on accurate forces, rather than energies. $T_s^{(2)}[\rho]$ is, however, less accurate than $T_s^{T92}[\rho]$, which is not unexpected given the simplicity of the form. The most accurate results are obtained using $T_s^{(3)}[\rho]$, although this is obtained at the expense of a violated density scaling condition.

It is interesting to test whether the functionals in this study bind diatomic molecules; relevant previous studies include the work of Karasiev et al.,[23,39] Iyengar et al.,[34] Constantin and Ruzsinszky,[35] Xia et al.,[9] and Chan et al.[40] It is well-known that $T_s^{TF}[\rho]$ cannot do this,[41] and this was illustrated in refs 23, 34, 35, and 39. Potential energy curves from the approximate functionals are obtained by simply replacing the Kohn–Sham $T_s[\{\phi_i\}]$ in the converged total electronic energy in eq 2 with the approximate $T_s[\rho]$.

The first diatomic we investigate is CO, allowing comparison with the work in ref 23. Figure 2a compares the potential energy curves with the Kohn–Sham curve. To aid comparison, Figure 2b and c align the curves at the largest bond length; note the change in the vertical scale. Our primary interest is whether binding is predicted, and so larger bond lengths are not considered. For clarity, the curves determined using $T_s^{(1)}[\rho]$, $T_s^{(2)}[\rho]$, and $T_s^{(3)}[\rho]$ (Figure 2b) have been plotted separately from those determined using $T_s^{TF}[\rho]$, $T_s^{T92}[\rho]$, and $T_s^{PBE2}[\rho]$ (Figure 2c).

The $T_s^{(1)}[\rho]$, $T_s^{(2)}[\rho]$, and $T_s^{(3)}[\rho]$ curves in Figure 2a reflect the observations in Figure 1. The $T_s^{(1)}[\rho]$ and $T_s^{(2)}[\rho]$ curves are too low and too high, respectively, whereas $T_s^{(3)}[\rho]$ provides a curve that is relatively close in energy to the Kohn–Sham curve. The $T_s^{TF}[\rho]$ and $T_s^{PBE2}[\rho]$ results are not visible on this scale, due to their large absolute errors. Figure 2b and c demonstrate that neither $T_s^{(1)}[\rho]$, $T_s^{(3)}[\rho]$, $T_s^{TF}[\rho]$, nor $T_s^{T92}[\rho]$ predict a bound molecule. By contrast, binding is predicted by $T_s^{(2)}[\rho]$ and $T_s^{PBE2}[\rho]$. We note that the $T_s^{(2)}[\rho]$ curve does exhibit a slight unphysical maximum at large bond lengths. The fact that PBE2 predicts binding is not surprising, given that the functional was specifically designed to reproduce accurate forces.

The same observations are made in the potential energy curves of F₂ in Figure 3, although the unphysical maximum in the $T_s^{(2)}[\rho]$ curve is much more pronounced. Results for the P₂
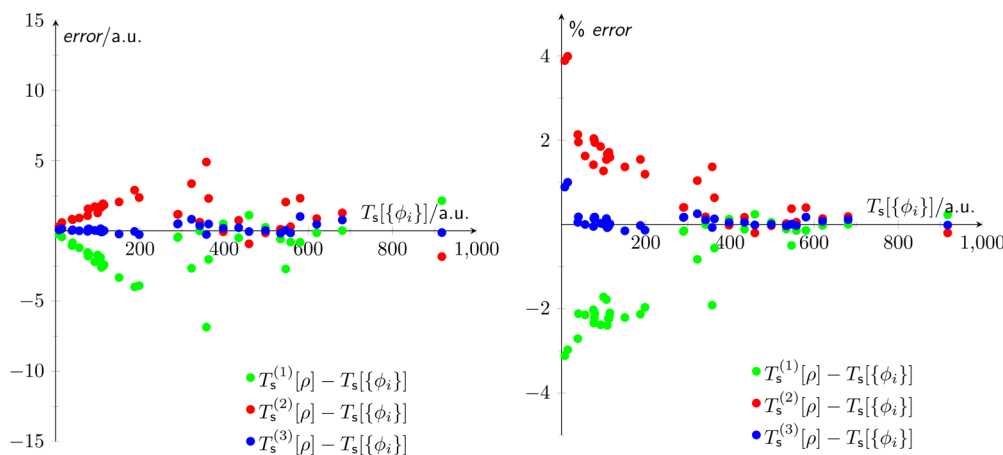
Figure 1. Errors and percentage errors in noninteracting kinetic energies, plotted as a function of $T_s[\{\phi_i\}]$, for the closed-shell molecules of the G1 set.
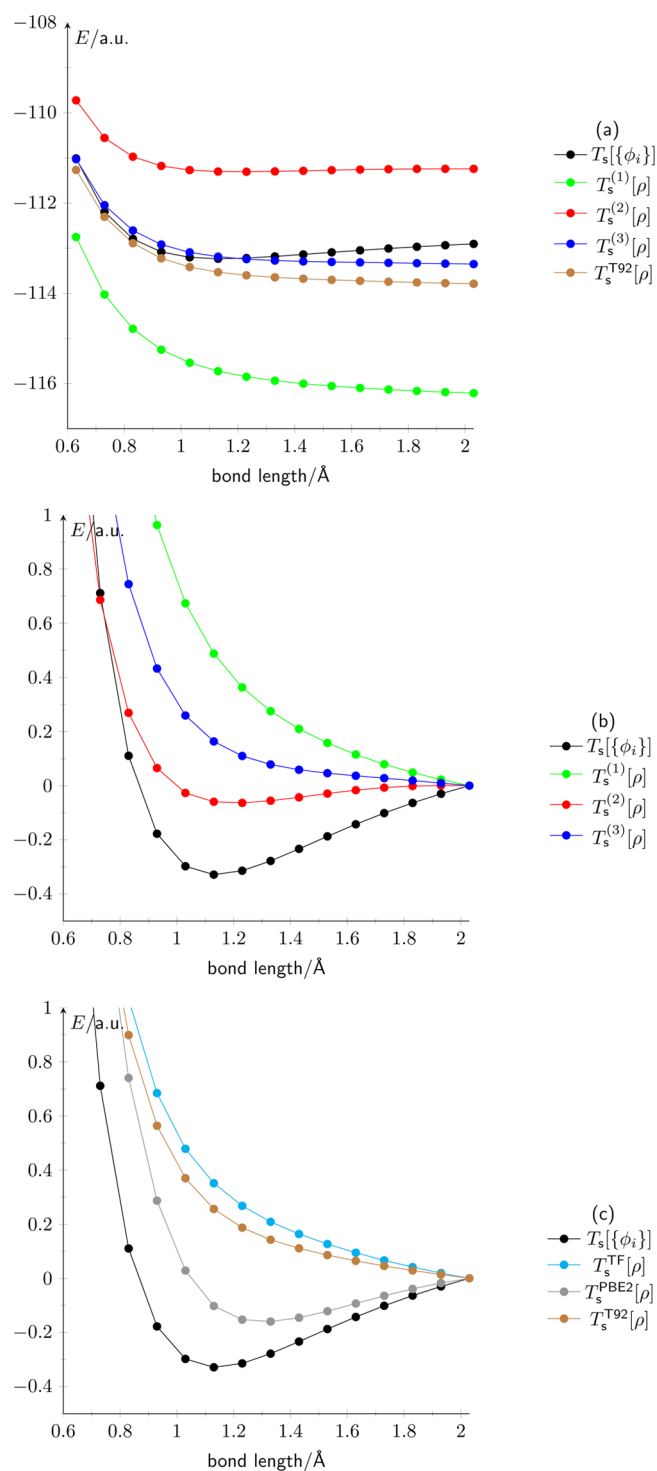
Figure 2. Potential energy curves of CO determined using various noninteracting kinetic energy functionals. See text for details.

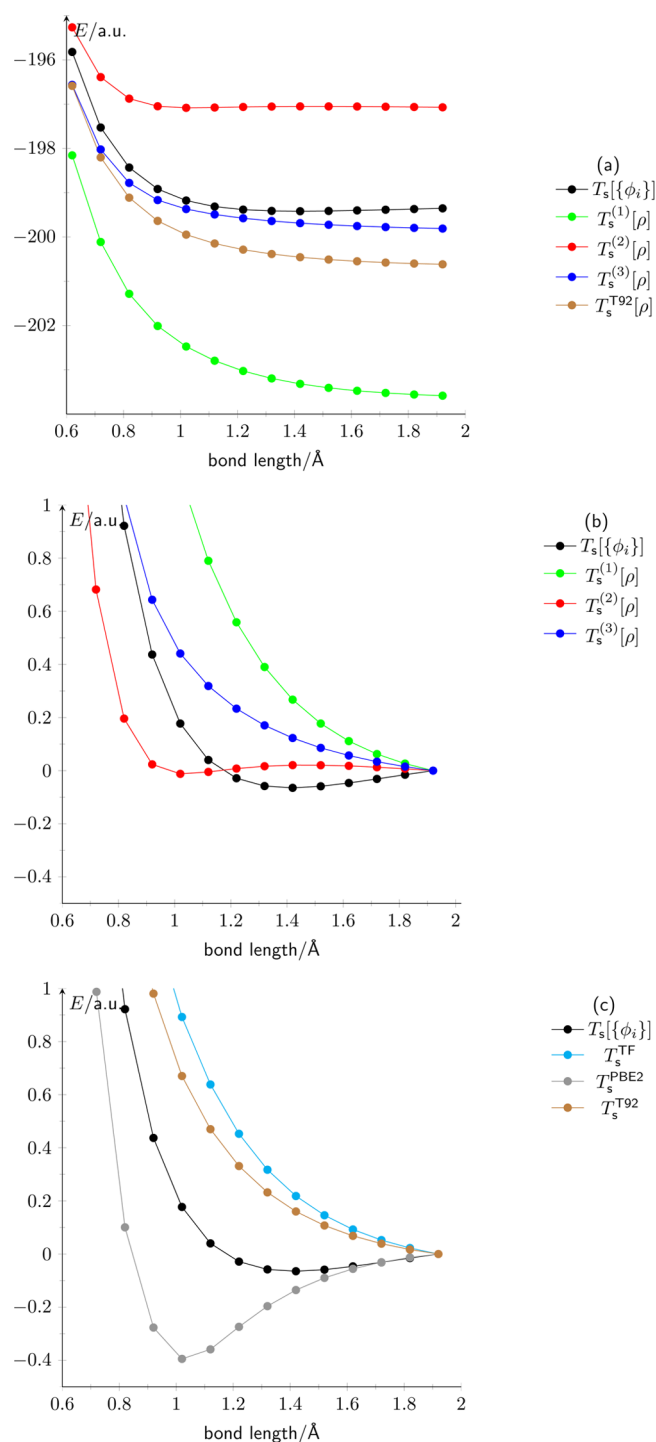**Figure 3.** Potential energy curves of F_2 determined using various noninteracting kinetic energy functionals. See text for details.

molecule are presented in Figure 4. In this case, binding is predicted by $T_s^{(2)}[\rho]$, $T_s^{(3)}[\rho]$, and $T_s^{PBE2}[\rho]$.

In addition to PBE2 and T92, we also determined the potential energy curves of the three molecules using a wide range of other published GGA functionals, namely LLP91,[10] LC94,[11] TW02,[12] PBE3 and PBE4,[13] APBEK and revAP-BEK,[14,15] E00,[16] P92,[17] OL1 and OL2,[18] PW86,[19] and PW91k.[20,21] With the exception of PBE3 and PBE4 (which,

like PBE2 were designed to reproduce accurate forces), none of the functionals predict any of the three molecules to be bound.

Notwithstanding the post-Kohn−Sham nature of the calculations and the lack of quantitative accuracy, we are encouraged that $T_s^{(2)}[\rho]$ predicts a bound molecule in all three cases, whereas $T_s^{(1)}[\rho]$ predicts purely repulsive curves. This suggests that imposing density scaling may be beneficial. Further support is provided by the fact that $T_s^{(3)}[\rho]$, which has the same flexibility as $T_s^{(2)}[\rho]$ but violates the density scaling condition in order to maximize energy accuracy, fails to bind
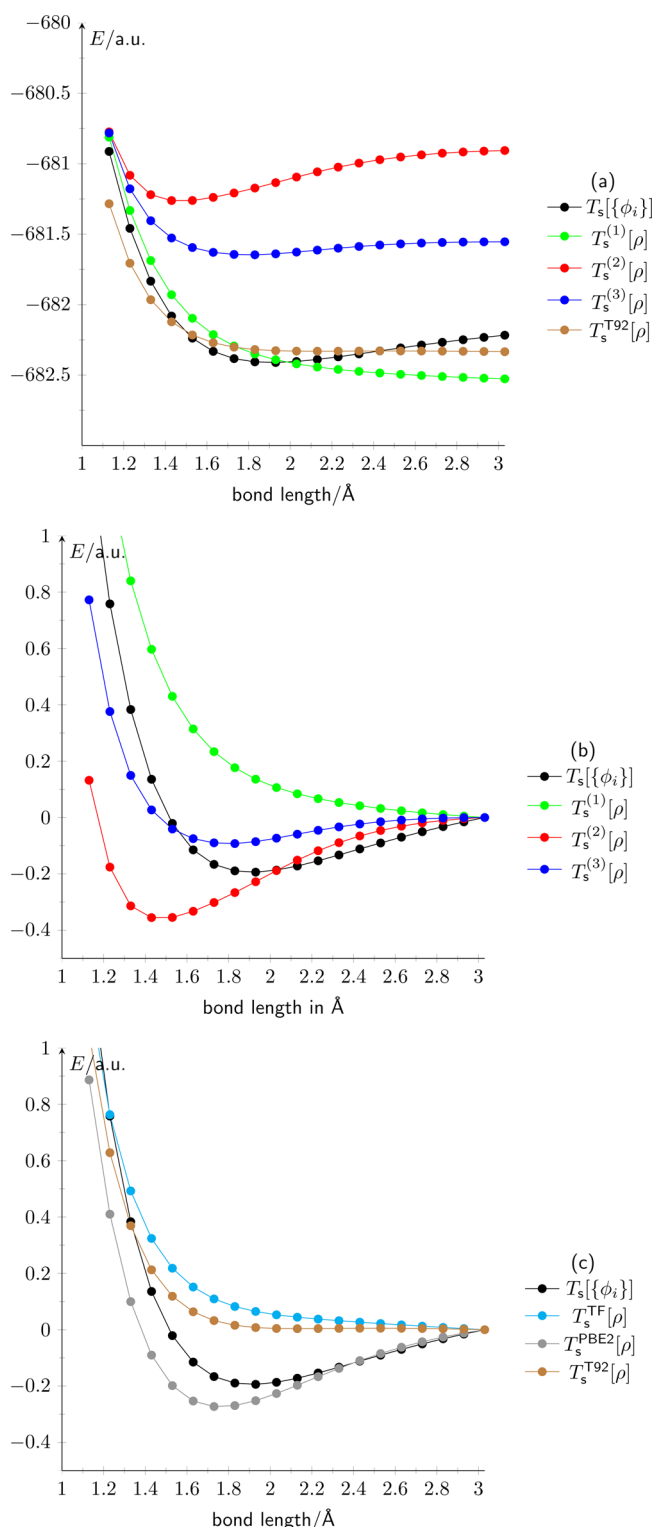
2253

dx.doi.org/10.1021/ct400129d | *J. Chem. Theory Comput.* 2013, 9, 2250−2255

Figure 4. Potential energy curves of P_2 determined using various noninteracting kinetic energy functionals. See text for details.

CO and F_2. The findings may reflect the fact that the density scaling condition involves both the noninteracting kinetic energy and its *potential*, see eq 7. For an approximate $T_s[\rho]$, the noninteracting kinetic potential is a key quantity in the Euler equation, which yields the corresponding electron density. This density, in turn, governs the accuracy of the nuclear forces through the Hellmann−Feynman theorem.[42] The noninteract-

ing kinetic potential is therefore a key quantity in determining the shape of a potential energy curve. Investigation of the Euler equation[9,39,40,43] associated with these approximate functionals is required, but is beyond the scope of the present study.

CONCLUSIONS AND FUTURE WORK

We have investigated the influence of imposing an approximate density scaling condition on a noninteracting kinetic energy functional. A simple GGA was presented, which satisfies both the density scaling condition and the usual coordinate scaling condition; the remaining multiplicative constant was determined from an energy criterion. In post-Kohn−Sham calculations, noninteracting kinetic energies of the closed-shell molecules of the G1 set from the GGA are a modest improvement over those determined using the corresponding local functional, which does not satisfy the density scaling condition. Potential energy curves of CO, F_2, and P_2 exhibit binding with the GGA, compared to purely repulsive curves with the local functional. Adjusting the exponent in the GGA form in order to optimize energy accuracy violates the density scaling condition, and two of the diatomics no longer exhibit binding. Results were compared with those from other local/GGA functionals in the literature.

The findings of this study suggest that imposing approximate density scaling may be beneficial, warranting further research. The form of $T_s^{(2)}[\rho]$ provides a simple way to impose a given homogeneity, but the form is of limited flexibility and cannot, for example, describe the uniform electron gas. More flexible forms must be considered. Other avenues of research include the study of the Euler equation associated with approximate functionals and the application of these functionals to more diverse sets of molecules. Investigations are underway.

AUTHOR INFORMATION

Corresponding Author
*E-mail: a.j.borgoo@durham.ac.uk, d.j.tozer@durham.ac.uk.
Notes
The authors declare no competing financial interest.

ACKNOWLEDGMENTS

REFERENCES

(1) Kohn, W.; Sham, L. J. *Phys. Rev.* **1965**, *140*, A1133−A1138.
(2) Parr, R. G.; Yang, W. T. *Density Functional Theory of Atoms and Molecules*; Oxford University: New York, 1989; pp 47−69.
(3) Wesolowski, T. A.; Warshel, A. *J. Chem. Phys.* **1993**, *97*, 8050−8053.
(4) Wesolowksi, T. A. In *Comp. Chem.: Reviews of Current Trends*; Leszczynski, J., Ed.; World Scientific: River Edge, NJ, 2006; Vol. *10*, pp 1−82.
(5) Götz, A. W.; Beyhan, S. M.; Visscher, L. *J. Chem. Theory Comput.* **2009**, *5*, 3161−3174.
(6) Fermi, E. *Rend. Accad. Naz. Lincei* **1927**, *6*, 602.
(7) Thomas, L. *Math. Proc. Cambridge Philos. Soc.* **1927**, *23*, 542−546.
(8) Smargiassi, E.; Madden, P. A. *Phys. Rev. B* **1994**, *49*, 5220−5226.
(9) Xia, J.; Huang, C.; Shin, I.; Carter, E. A. *J. Chem. Phys.* **2012**, *136*, 084102.

(10) Lee, H.; Lee, C.; Parr, R. G. *Phys. Rev. A* **1991**, *44*, 768−771.

(11) Lembarki, A.; Chermette, H. *Phys. Rev. A* **1994**, *50*, 5328−5331.

(12) Tran, F.; Wesołowski, T. A. *Int. J. Quantum Chem.* **2002**, *89*, 441−446.

(13) Karasiev, V.; Trickey, S.; Harris, F. *J. Comput.-Aided Mater. Des.* **2006**, *13*, 111−129.

(14) Laricchia, S.; Fabiano, E.; Constantin, L. A.; Della Sala, F. *J. Chem. Theory Comput.* **2011**, *7*, 2439−2451.

(15) Constantin, L. A.; Fabiano, E.; Laricchia, S.; Della Sala, F. *Phys. Rev. Lett.* **2011**, *106*, 186406.

(16) Ernzerhof, M. *J. Mol. Struct.: THEOCHEM* **2000**, *501−502*, 59−64.

(17) Perdew, J. P. *Phys. Rev. A* **1992**, *165*, 79−82.

(18) Ou-Yang, H.; Levy, M. *Int. J. Quantum Chem.* **1991**, *40*, 379−388.

(19) Perdew, J. P.; Wang, Y. *Phys. Rev. B* **1986**, *33*, 8800−8802.

(20) Perdew, J. P.; Chevary, J. A.; Vosko, S. H.; Jackson, K. A.; Pederson, M. R.; Singh, D. J.; Fiolhais, C. *Phys. Rev. B* **1992**, *46*, 6671−6687.

(21) Lacks, D. J.; Gordon, R. G. *J. Chem. Phys.* **1994**, *100*, 4446−4452.

(22) Thakkar, A. J. *Phys. Rev. A* **1992**, *46*, 6920−6924.

(23) Karasiev, V. V.; Jones, R. S.; Trickey, S. B.; Frank, E. H. In *New Developments in Quant. Chem.*; Paz, J. L., Hermández, A. J., Eds.; Transworld Research Network: Trivandrum, Kerala, India, 2009; Chapter 2, pp 25−54.

(24) Levy, M.; Perdew, J. P. *Phys. Rev. A* **1985**, *32*, 2010−2021.

(25) Borgoo, A.; Teale, A. M.; Tozer, D. J. *J. Chem. Phys.* **2012**, *136*, 034101.

(26) Liu, S.; Parr, R. G. *Phys. Rev. A* **1996**, *53*, 2211−2219.

(27) Zhao, Q.; Morrison, R. C.; Parr, R. G. *Phys. Rev. A* **1994**, *50*, 2138−2142.

(28) von Weizsäcker, C. *Z. Phys. A* **1935**, *96*, 431−458.

(29) Oliver, G. L.; Perdew, J. P. *Phys. Rev. A* **1979**, *20*, 397−403.

(30) Perdew, J. P.; Burke, K.; Ernzerhof, M. *Phys. Rev. Lett.* **1996**, *77*, 3865−3868.

(31) Dunning, T. H. *J. Chem. Phys.* **1989**, *90*, 1007−1023.

(32) Kendall, R. A.; Dunning, T. H.; Harrison, R. J. *J. Chem. Phys.* **1992**, *96*, 6796−6806.

(33) Woon, D. E.; Dunning, T. H. *J. Chem. Phys.* **1993**, *98*, 1358−1371.

(34) Iyengar, S. S.; Ernzerhof, M.; Maximoff, S. N.; Scuseria, G. E. *Phys. Rev. A* **2001**, *63*, 052508.

(35) Constantin, L. A.; Ruzsinszky, A. *Phys. Rev. B* **2009**, *79*, 115117.

(36) Perdew, J. P.; Levy, M.; Painter, G. S.; Wei, S.; Lagowski, J. B. *Phys. Rev. B* **1988**, *37*, 838−843.

(37) Handy, N. C.; Tozer, D. J. *Mol. Phys.* **1998**, *94*, 707−715.

(38) Borgoo, A.; Tozer, D. J. *J. Phys. Chem. A* **2012**, *116*, 5497−5500.

(39) Karasiev, V.; Trickey, S. *Comput. Phys. Commun.* **2012**, *183*, 2519−2527.

(40) Chan, G. K.-L.; Cohen, A. J.; Handy, N. C. *J. Chem. Phys.* **2001**, *114*, 631−638.

(41) Teller, E. *Rev. Mod. Phys.* **1962**, *34*, 627−631.

(42) Feynman, R. P. *Phys. Rev.* **1939**, *56*, 340−343.

(43) Yonei, K. *J. Phys. Soc. Jpn.* **1971**, *31*, 882−894.